PROJECT OF UNIVERSAL TEST STAND FOR UNDERWATER VEHICLES' THRUSTERS

Filip Dudek[1]*, Patrycja Lisak[2], Piotr Makulec[3], Tomasz Małachowski[4], Krzysztof Piekorz[5], Kacper Przybylski[6], Bartłomiej Borkowski[7]

AGH University of Science and Technology, Mickiewicza 30, 30-059, Cracow, Poland
[1] e-mail: filipodu982@gmail.com, ORCID 0000-0002-1007-9256
[2] ORCID 0000-0002-5404-9251
[3] ORCID 0000-0001-6132-6109
[4] ORCID 0000-0003-1611-9519
[5] ORCID 0000-0001-9831-0880
[6] ORCID 0000-0002-7896-3048
[7] ORCID 0000-0003-4339-1358
*Corresponding author

Abstract: This article presents the design and implementation of the next stage of research conducted as part of the design and construction of an underwater inspection robot. Its purpose was to create a universal test stand for testing the parameters of underwater robots' thrusters. Factors taken into account when constructing the station were, among others, the possibility of cavitation and its impact on the strength of the device's thruster system, as well as noise pollution of the underwater environment. The sensor system in which the dynamometer is equipped will automatically acquire a number of readings that will allow the design of propulsors to be tested taking into account many parameters. The collected data is sent and analysed using microcontrollers and dedicated, custom-written software. The proposed solution will accelerate and automate research work and allow quick modifications of the mathematical model for describing the underwater vehicle propulsion module.

Keywords: thrusters, ROV, test stand, propellers, propulsion.

1. INTRODUCTION

ROVs (Remotely Operated Vehicles) and AUVs (Autonomous Underwater Vehicles) are types of robots that perform various types of underwater work. Thanks to the precise thrusters, manipulators, the whole spectrum of sensors and vision systems, these vehicles are used in many branches of industries and science – from environmental research, through the installation of mining equipment, to military applications [Antonelli 2016].

In order to eliminate the negative impact of ROVs and AUVs on the natural environment and, above all, to improve their operating parameters, it becomes

necessary to optimise the propulsion systems in terms of heat, noise and cavitation [Richardson et al. 1995], as well as the selection of such operating parameters and geometry that the efficiency is as high as possible. The construction of a multi-purpose test stand for testing robot thrusters was therefore a key task to perform to consequently carry out the ROV, and later AUV, project which will not have a negative impact on the environment and will be characterised by high efficiency, mechanical strength and low electricity consumption.
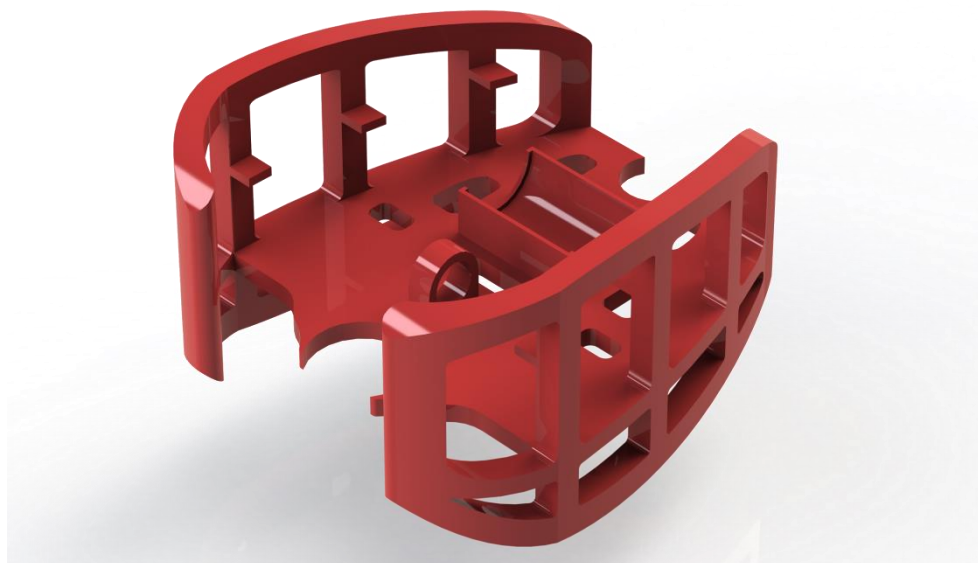
Fig. 1. The concept and example of the structure of an underwater robot
with designated places for the assembly of accessories [Małachowski et al. 2019]

A ROV's thrusters are one of the most important peripherals of the robot, which determine its speed, controllability, stability, capacity and pull. Their work ensures mobility, counteracts water currents, and determines the depth and rotation of the robot. They are also the modules that consume the most energy. This is especially important in the case of AUVs that use only power from internal batteries.

The thruster consists of three main elements: propeller, motor and nozzle. The propellers are exposed to damage resulting from collisions with other objects or caused by the phenomenon of cavitation. Their work and the possible occurrence of cavitation also cause noise, which is harmful to the marine environment, as well as to the sensors which are sensitive to sound and vibration [Aktas et al. 2018]. Each rotating object and the motor running also cause vibrations that are unfavourable to all systems, i.a. due to resonance phenomena that may occur. Based on analyses in the ANSYS Fluent program [ANSYS, Inc. 2013] and thanks

to the scientific literature, it was also concluded that the phenomenon of cavitation may occur, and consequently the generation of cavitation noise. The intensity and presence of this phenomenon largely depend on the number and geometry of the blades, the rotational speed of the propeller, the ambient temperature, and the depth of operation [Andersen, Kappel and Spangenberg 2009].

2. TEST STAND DESIGN GUIDELINES

For the above reasons, it is very important for optimising the ROV's structure in terms of efficiency, to choose the best parameters of the propeller and the entire thruster, perform simulations and then confirm the real work characteristics, as these usually differ from the simulated ones. The next step is therefore to verify these relationships experimentally. To do this, it was decided to construct a test stand equipped with a number of sensors, thanks to which we are able to learn the whole range of characteristics of a given thruster unit and choose the best solution for the project. The task of the test stand is to register parameters such as:

- current consumption – finding out the real power consumption of the thruster;
- actual rotational speed and torque – calculation of the power transmitted by the thruster;
- real thrust – calculation of efficiency and the relationship between rotational speed and thrust;
- temperature – preventing overheating of the structure and measuring the effect of temperature on cavitation;
- vibration – minimising the negative impact of vibration on a structure that can be damaged and on the environment;
- noise level – acoustic analysis of the phenomenon of cavitation and the impact of noise on the aquatic environment;
- pressure – the lower the pressure, the lower the boiling point of water, which facilitates the occurrence of cavitation.

A detailed analysis of the above quantities using a test stand is a necessary step to make an accurate mathematical model of the thruster, and then use this description for precise simulations and further design work on the ROV drive system. Below is a diagram of the connection of the control station with the control unit (Fig. 2).
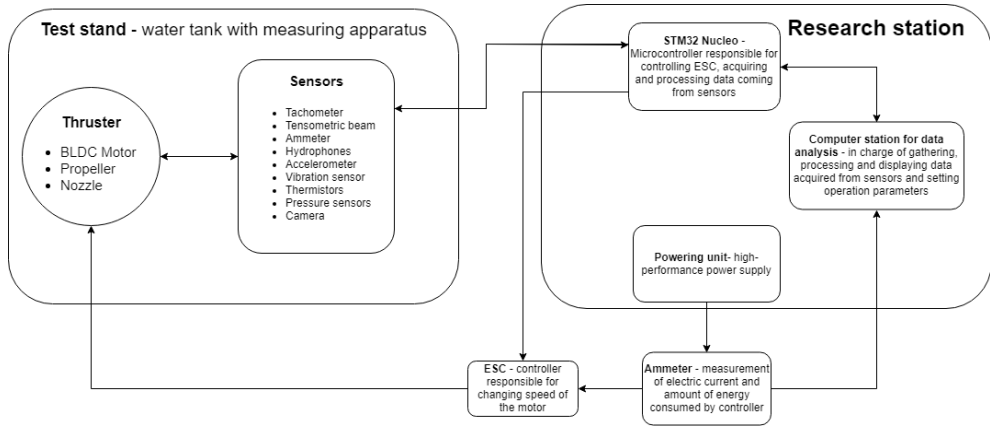
Fig. 2. Diagram of the station and connections between individual modules
[Małachowski et al. 2019]

3. MECHANICAL CONSTRUCTION

When creating the test stand, a 1010x1205x550 mm water tank was used (Fig. 3), which will be the main working environment.
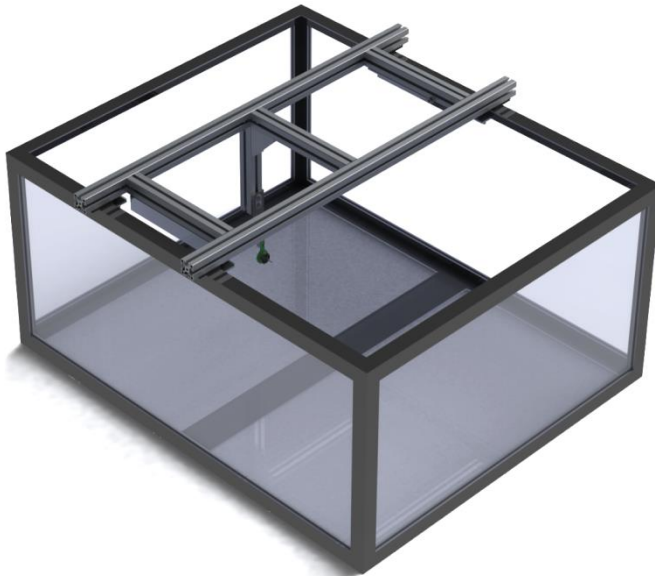
Fig. 3. 3D model of the test stand mounted on the main tank [Małachowski et al. 2019]

The frame concept assumes the possibility of being mounted on tanks of various sizes and at different depths, which makes the solution universal. A frame made of aluminium profiles was also made, on which the sensors are placed. To enable reliable measurements of different thrusters, it is important to position them at the same point. Due to the fact that the sizes of individual motors differ, it has become necessary to create a special assembly (Fig. 4) for connecting the motors and dedicated fixtures that will regulate the height at which the propeller is located.

Fig. 4. 3D model of the dynamometer structure from below, with motor mounting in the foreground [Małachowski et al. 2019]

4. ELECTRONIC SYSTEM AND SENSORS

Data acquisition is carried out using a set of microcontrollers, consisting of an STM32 Nucleo-144 board, which is the centre of the sensor system, and an STM32 Nucleo-64 board, whose task is to operate the temperature sensor and communicate with the other device. In order to ensure the accuracy of measurements and that their precision does not change over time, calibration functions have been added to the software that reduce measurement errors before each test. Thanks to them, information on the correct operation of the entire measuring system is obtained. In addition to data acquisition, the microcontroller is also responsible for setting the operating parameters of the propeller, thanks to the PWM (Pulse Width Modulation) signal control sent to the ESC (Electronic Speed Controller). The ESC itself is powered by a 600W laboratory power supply unit. This allows for precise testing of various levels of the thruster's work, i.e. maximum rotational speed,

current consumption, efficiency, torque and thrust, and then selection of the best solution for use in ROV design.

4.1. Microcontroller

In the dynamometer design, it was decided to use an STM32 Nucleo-144 board with an STM32F767ZI processor [STMicroelectronics 2017] with a clock frequency of 216 MHz, and an STM32 Nucleo-64 with an STM32F446RE computation unit [STMicroelectronics 2016] with a lower clock frequency of 180 MHz. Both are equipped with three 12-bit A/D converters, two D/A, a real-time clock with low power consumption, twelve 16-bit general purpose clocks, of which two have the ability to generate PWM (Pulse Width Modulation) signals to regulate motor speed, two general purpose 32-bit clocks, a random number generator, and communication interfaces such as: I2C, UART/USART, SPI, CAN, USB, and Ethernet. In addition, they have ST Zio and ST Morpho connectors connected with processor pins, which can serve, for example, as GPIO pins (General Purpose Input/Output). The more efficient device performs the task of acquiring all data, processing them and communicating with the control station and also with a second board via the UART interface. The second microcontroller deals with operating the temperature sensor, which, due to its data transmission interface, significantly loads the processor, which in the case of using only one board was associated with a long delay in data transmission.

4.2. Tachometer

A UT372 meter [Shimana 2019] is able to check the real motor speed. The principle of work of this sensor is based on measuring the number of reflections of a laser beam from the measuring surface – a reflective sticker – in a given unit of time, and then providing the result in revolutions per minute (RPM). Knowledge of the motor speed is important because it is closely related to the efficiency of the motor itself as well as the propeller and the entire thruster system.

4.3. Load cell

A load cell was used to measure the thrust [Electronicos Caldas 2013] placed on an aluminium profile perpendicularly to the thrust, together with a HX711 amplifier (Fig. 5). Its sampling frequency is 10 Hz, which is dictated by the hardware restrictions of the amplifier circuit itself [Avia Semiconductor (Xiamen) Co., Ltd. 2012]. The basic element of the cell is a resistance strain gauge whose resistance varies depending on its elongation caused by the application of force to the cell.

Then, by using a Wheatstone bridge, the resistance change value is read, which is amplified and converted into a digital signal by the HX711 amplifier and a 24-bit analog-to-digital converter (ADC), which provides us with a resolution of 0.3 µV.

Data processed in this way can be sent to the Nucleo-144 via a two-wire bus – data line and clock. This forces the use of a dedicated library to support the sensor, due to the need to send high and low states in the right configuration on a clock line of the appropriate duration while at the same time reading the transmitted bits on the data line. The reading itself is not scaled in any unit. Only the calibration functions convert the raw data from the analog-to-digital converter located on the HX711 into SI units. To ensure the accuracy of measurements, calibration takes place before each test and consists of zeroing the sensor reading and then applying a force of known value and using this information in the data conversion process. During the first tests, it turned out that the adhesive used by the manufacturer to attach the strain gauge to the beam is not waterproof, which led to flooding of the sensor and erroneous readings. To prevent this, the surface was sealed with a thin waterproof coating that does not affect the measurement.

4.4. Shunt and Hall sensor

In order to measure the efficiency of the entire thruster system, current consumption is measured in two places – at the output of the power unit by a shunt, and between the ESC and the BLDC motor using a Hall sensor [Allegro MicroSystems, LLC 2019].

The shunt is a resistor with a very small resistance value (3 mΩ) selected so that the voltage drop on it does not affect the operation of the motor. Thanks to the LM358 operational amplifier and a properly designed electrical system, this drop is measured, amplified and transmitted to the analog-to-digital converter on the Nucleo-144. Amplification is necessary because the 12 bit resolution of the converter is insufficient to measure very small voltage drops. Without the use of the amplifying system, the shunt accuracy is + -0.2 A, which is unsatisfactory. This system allows the precision to be increased to + -0.01 A. The value obtained after conversion is not scaled in any unit. Only after conversion, data in amperes are sent to the control unit. To eliminate errors, the whole system was previously calibrated by measuring the applied current with an electric meter and determining the proportionality coefficients between the expected and the obtained values.

The principle of the sensor is based on the Hall effect. The current flowing through the conductor generates a magnetic field whose magnitude is proportional to the amount of current flowing. The sensor determines the value of the surrounding magnetic field and sends it to an analog-to-digital converter on the Nucleo-144 board with a frequency of 10 kHz, which means that it can be

effectively measured to a frequency of about 2 kHz. Proprietary software then converts it into current scaled in amperes and passes it to the control unit.

This arrangement of sensors is the result of the stand's tests. It turns out that the shunt system we designed was not able to accurately measure the alternating current generated by the ESC. The Hall sensor does not have such disadvantages and accurately reads the value of the current regardless of its variability in time.

4.5. Vibration sensor

To measure vibration, a piezoelectric vibration sensor was used, sampled at 10 kHz, with additional mass to improve the quality of readings at lower frequencies [TE Connectivity 2019]. Its sensitivity is at the level of 1.1 V/g, which means that the amplitude of the electrical impulses generated by it can reach even + -90 V. To minimise the risk of damage done to the STM32 Nucleo-144 board, the use of a high-value resistor is necessary. The sensor's electrical capacity of 244 pF causes the parallel connection to the resistor to create a high-pass filter, which may result in the inability to measure low-frequency vibration. Therefore, a system of resistors with a total resistance of 154 MΩ was selected, which gives a filter cut-off frequency of about 4.2 Hz, i.e. 252 RPM of the engine. This number is sufficient to examine the vibration level over the entire spectrum of engine speeds, as these are usually between 300 RPM and over 4000 RPM [Blue Robotics 2014].

Then, as in the case of the shunt, to increase the accuracy of measurements, a differential amplifier system was designed, which in addition to amplifying the signal also shifts it in the vertical axis. The analog-to-digital converters on the Nucleo-144 board do not read negative voltages, which in the case of an alternating signal generated by the sensor would mean the loss of half the information. To do this, adding an offset that allows the entire signal to be read and properly analysed is needed.

4.6. Temperature sensors

The temperature of the water in the tank is closely related to cavitation. The higher the temperature, the easier it is to observe this phenomenon. In addition, thermal control provides information on potential overheating of the thruster system. The test stand uses two DS18B20 temperature sensors [Maxim Integrated 2019] – one at the motor and the other at a distance from it. These sensors are very popular, precise and, most importantly, waterproof. They communicate with the STM32 Nucleo-64 via a 1-wire interface.

This method of communication is characterised by a high degree of complexity – it requires sending high and low states on a data line, reading transmitted bits and then bit shifts. This results in a high load on the

microcontroller and a long readout time of the level of up to several dozen milliseconds. Initially, the DS18B20 sensors were connected together with other sensors to the STM32 Nucleo-144, but tests revealed a significant delay in data transmission.

This observation was the reason that a second board was implemented, dedicated only to temperature reading, with UART communication between the controllers. Thanks to this, data transfer to the control unit happens in real-time. Before installing the sensors in the test stand, they were calibrated by comparing the temperature of boiling water and ice-water mixtures with the sensor readings.

4.7. Hydrophone

To measure the sound level generated by the propeller, a H2A Hydrophone [Aquarian Hydrophones 2019] was used. It has a frequency range from about 10 Hz to 100 kHz, and can be submerged to a depth of about 80 m. The hydrophone is connected directly to a computer compatible with the control station via a 3.5 mm minijack microphone input. In addition to measuring sound intensity, the acoustic signal is subjected to Fourier analysis in real-time.

The phenomenon of cavitation increases the power spectral density in a certain frequency range, depending on, among others, the type of this phenomenon [Aktas et al. 2018].

This increase can be detected during the experiment as an increased amplitude in the frequency domain chart, which may suggest cavitation. However, further analysis of the material from the video recorder will be needed to confirm this hypothesis.

4.8. Camera

Cavitation is a phenomenon whose intensity can be observed visually. To do this, we use a SJCAM M20 camera with a waterproof housing [SJCam Limited 2019].

This device can work without interruption for a maximum of 75 minutes, recording images even at a resolution of 4K and with a viewing angle of up to 166 degrees. The housing allows the camera to be submerged to a depth of 30 m. These parameters allow the real-time motion of the propeller being tested in the dynamometer to be recorded in high resolution and the formation of cavitation on the propeller to be visually determined.
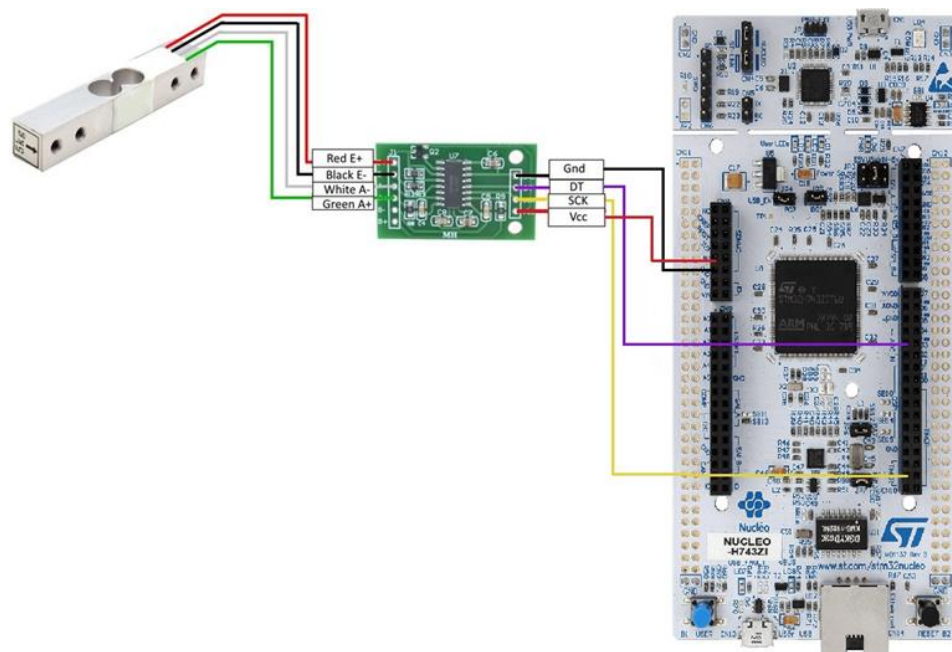
Fig. 5. Connection diagram of the load cell with the HX711 amplifier and microcontroller
[Małachowski et al. 2019]

5. CONTROL STATION SOFTWARE

Each measurement system requires a built-in or separate agglomeration, data processing and representation system, as well as set of test parameters. Due to the basic lack of such solutions on the market, in the case of the test stand being constructed, it became necessary to create our own software supporting the work of the station.

The developed system can be divided into two main components. The first is the STM32 microcontroller software located on the Nucleo-144 and Nucleo-64 boards. The program was created in the Embedded C language, which is a typical solution for such tasks [International Organization for Standardization/International Electrotechnical Commission 2008]. The scheme of operation of the software is based on cyclic interrupts triggered by timers, through which specific actions are performed – reading the sensor status, communication between boards or with a computer. When creating software that works in real-time, it was ensured that the microcontroller was clocked properly and the procedures performed were not too complex to be completed within the allotted time.

The main assumption while designing the software for the computer being the centre of the test stand was the ability to quickly handle large, as for personal

computers, amounts of data flowing from the microcontroller, hydrophone, tachometer, and camera. Data from the microcontroller is delivered to the computer via a serial port emulated in a USB connector [Compaq Computer Corporation; Hewlett-Packard Company; Intel Corporation; Lucent Technologies Inc; Microsoft Corporation; NEC Corporation; Koninklijke Philips Electronics NV 2000] or an Ethernet port, the hydrophone is connected to the computer's sound card, the tachometer through a separate USB port via the HID interface, and the camera is connected to a separate USB port. The Nucleo-144 board transmits the data set every 1 millisecond, the tachometer every 100 milliseconds, the hydrophone is sampled with the maximum sampling frequency of the sound card built into the computer that supports the test stand, which in this case is 44 100 Hz, and the most typical video camera setting is 1920x1080 pixels at 60 frames per second. Due to the assumed high performance of the program, it was decided to use the C++ language.

Data on the microcontroller are stored in the appropriate floating-point variables. In order to transfer this data to a computer, it is converted into frames that organise values relative to a pre-determined key, and then sent to the station. Sample frame scheme:

<minutes | seconds | milliseconds | temperature | thrust | shunt current | vibration value table | Hall sensor current table>

During the software development, two key difficulties related to communication between the Nucleo-144 board and the computer were solved.

The first problem was related to the accurate determination of the time when the microcontroller measured a value. The most obvious solution was to check the system time when receiving a data frame from the microcontroller, however the Windows operating system is not a real-time system and these measurements would not be accurate. Also, due to the time needed for communication protocols to convert and transfer data via USB/COM, random delays would significantly affect the accuracy of the measuring signal sampling time. While this is not very important for measurements such as thrust or DC current from the power supply, it prevents the correct processing or interpretation of signals oscillating in time – vibration and current flowing from the ESC to the motor. It was therefore decided that the Nucleo-144 board would be responsible for measuring the times. The STM32F767ZI microcontroller is able to measure time at 100 microsecond intervals with an error of less than 1% [STMicroelectronics 2017] thanks to the clock and bus clocking with meters from the internal resonator meters at 200 MHz [STMicroelectronics 2017]. The measurement time is saved and sent in a data frame, and then used for the presentation and processing of the data.

The second difficulty is the data transmission. With some sensors turned on, data is transmitted at a rate of about 100–200 kilobits per second, which can be done without loss and interference. With all active sensors, the program has to send dozens of floating point values every millisecond, which equates to 1.5–2 megabits

of data per second, and may exceed the serial port throughput [YUKO Computer Plant 2019]. The solution then is the Ethernet port, where the transmission speed is much higher – up to 100 megabits per second, and which the Nucleo-144 board is equipped with.

The application represents all collected values in graphical form on charts, in the case of vibration, noise level and current values, and also calculates the values obtained from the microcontroller and scales the chart. After completing the measurement, it is possible to export this data to files that can be imported into spreadsheets or used in presentations. The program window also has controls that perform predefined functions that allow users to control the work of the station.

The second window presents the measurement of the signal from the hydrophone, the Fourier transform of this signal, and the spectrogram. The transform is calculated using the FFTW (Fastest Fourier Transform in the West) library function from 2048 samples taken at 44 100 Hz. FFTW is the fastest free library that performs Fourier transform [Frigo and Johnson 2019]. The spectrogram is created from the representation on the bitmap of Fourier analysis of subsequent time steps. An important issue to keep in mind with DFT algorithms is spectrum leaks that distort the result. To address this, a time window was used. A Blackman window was used, which has good dynamic characteristics and high resolution [Harris 1987].
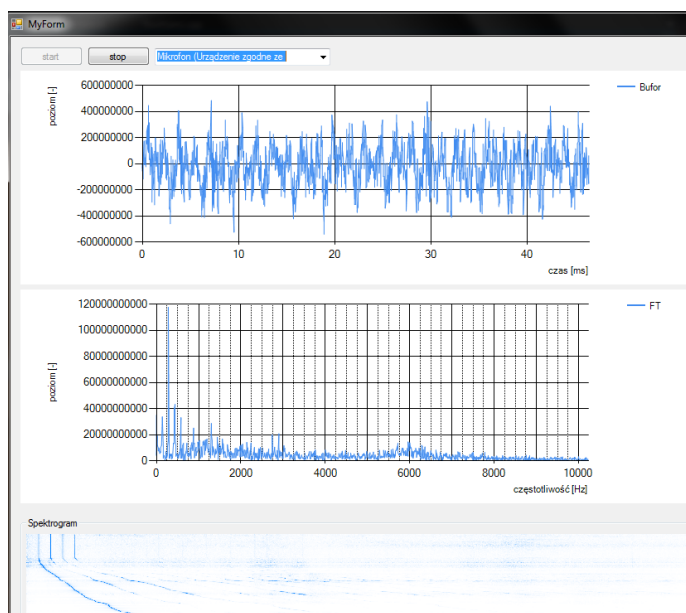
Fig. 6. Screenshot from the second application window for presenting results collected using the test stand

Source: own study.

6. SUMMARY

The test stand designed and built by the AGH Marines Science Club provides precise and reliable data, thanks to which comprehensive research and analyses can be carried out in a short time. This significantly speeds up work on the thruster system, where optimisation in terms of performance and minimising the impact on the environment as well as appropriate performance, increases the chances of faster creation of an innovative and technologically advanced ROV. Hence, the project of a multi-purpose test stand for underwater vehicles is a milestone on the way to the start of AGH Marines at the MATE ROV Competition [MATE 2019]. The test stand was created as part of the "Rector's Grant" 2019. The next stage will be the full use of the test stand in testing various propeller solutions by choosing the best thruster system of the designed ROV.

REFERENCES

Aktas, B., Atlar, M., Fitzsimmons, P., Shi, W., 2018, *An Advanced Joint Time-Frequency Analysis Procedure to Study Cavitation-Induced Noise by Using Standard Series Propeller Data*, Ocean Engineering, vol. 170, pp. 329–350.

Allegro MicroSystems, LLC 2019, *Hall Sensor – Datasheet*, Allegro MicroSystems, Manchester, New Hampshire, USA, https://www.pololu.com/file/0J497/ACS711.pdf, viewed 25 May 2019.

Andersen, P., Kappel, J.J., Spangenberg, E., 2009, *Aspects of Propeller Developments for a Submarine*, Proceedings of the First International Symposium on Marine Propulsors – smp'09, First International Symposium on Marine Propulsors, Trondheim, Norway, pp. 554–562.

ANSYS, Inc. 2013, *ANSYS Fluent User's Guide*, ANSYS INC., Canonsburg, Pennsylvania, USA, http://www.pmt.usp.br/ACADEMIC/martoran/NotasModelosGrad/ANSYS%20Fluent%20Users%20Guide.pdf, viewed 2 December 2018.

Antonelli, G., 2016, *Underwater Robots*, Springer, Berlin, Germany.

Aquarian Hydrophones, 2019, *H2a Hydrophone User's Guide*, Anacortes, Washington, USA, http://www.aquarianaudio.com/AqAudDocs/H2a_manual.pdf, viewed 25 May 2019.

Avia Semiconductor (Xiamen) Co., Ltd., 2012, *HX711 – datasheet*, Xiamen, China, https://cdn.sparkfun.com/datasheets/Sensors/ForceFlex/hx711_english.pdf, viewed 25 May 2019.

Blue Robotics, 2014, *T100 Thruster – Blue Robotics*, Blue Robotics, Torrance, California, https://www.bluerobotics.com/store/thrusters/t100-t200-thrusters/t100-thruster/, viewed 26 May 2019.

Compaq Computer Corporation; Hewlett-Packard Company; Intel Corporation; Lucent Technologies Inc; Microsoft Corporation; NEC Corporation; Koninklijke Philips Electronics N.V., 2000, *Universal Serial Bus Specification*, USB Implementers Forum, Inc., n.p., https://www.usb.org/document-library/usb-20-specification, viewed 20 May 2019.

Electronicos Caldas, 2013, *Loadcell – datasheet*, Manizales, Colombia, https://www.electronicoscaldas.com/datasheet/YZC-131A.pdf, viewed 25 May 2019.

Frigo, M., Johnson, S.G., 2019, *BenchFFT*, MIT, USA, http://www.fftw.org/benchfft/, viewed 15 May 2019.

Harris, F.J., 1987, *Handbook of Digital Signal Processing*, Chapter 3 – Multirate FIR Filters for Interpolating and Desampling', in DF Elliott (ed.), Academic Press, Anaheim, California, USA.

International Organization for Standarization/International Electrotechnical Commission, 2008, *Programming languages - C - Extensions to support embedded processors*, ISO/IEC TR 18037:2008, http://www.open-std.org/jtc1/sc22/wg14/www/docs/n1169.pdf, viewed 27 May 2019.

Małachowski, T., Lisak, P., Dudek, F., Stemplewski, M., Przybylski, K., Piekorz, K., Makulec, P., Borkowski, B., 2019, *Projekt wielozadaniowej hamowni napędów pojazdów podwodnych*, Materiały konferencyjne XXIII Konferencji inżynierii akustycznej i biomedycznej, Kraków-Zakopane, Poland.

MATE, 2019, The Marine Advanced Technology Education Center, Monterey Peninsula College, Monterey, California, USA, https://www.marinetech.org/rov-competition-2/, viewed 28 May 2019.

Maxim Integrated, 2019, *DS18B20 – Datasheet*, San Jose, California, USA, https://datasheets.maxim integrated.com/en/ds/DS18B20.pdf, viewed 25 May 2019.

Richardson, W.J., Greene Jr., C.R., Malme, C.I., Thomson, D.H. 1995, *Marine Mammals and Noise*, Academic Press, San Diego, California, USA.

Shimana, 2019, *UT372 Operating Manual*, Digital Measurement Metrology, Inc., Ontario, Canada, http://www.processinstruments.ca/store/index.php?page=shop.getfile&file_id=140&product_id =285&option=com_virtuemart&Itemid=46, viewed 26 May 2019.

SJCam Limited, 2019, *SJCam – Sklep internetowy*, Shenzen, China, https://sjcamhd.com.pl/kamery-sjcam/kamera-sportowa-sjcam-m20-pl1.html, viewed 25 May 2019.

STMicroelectronics, 2016, *Description of the STM32F446xC/E products*, Geneva, Switzerland, https://www.st.com/resource/en/datasheet/stm32f446re.pdf, viewed 25 May 2019.

STMicroelectronics, 2017, *Description of STM32F767xx devices*, STMicroelectronics, Geneva, Switzerland, https://www.st.com/resource/en/datasheet/stm32f767zi.pdf, viewed 25 May 2019.

TE Connectivity, 2019, *Vibration sensor – Datasheet*, Schaffhausen, Switzerland, https://www.te.com/commerce/DocumentDelivery/DDEController?Action=showdoc&DocId=D ata+Sheet%7FPiezo_Minisense_100-NM%7FA1%7Fpdf%7FEnglish%7FENG_DS_Piezo_ Minisense_100-NM_A1.pdf%7FCAT-PFS0011, viewed 25 May 2019.

YUKO Computer Plant, 2019, *Standard interfejsu RS 232C (V.24)*, Zakład Komputerowy YUKO, Gliwice, Poland, http://www.yuko.com.pl/v24b11.pdf, viewed 20 May 2019.